2 GeV Electron Beam Irradiation Effects in Advanced Metallic Glasses

Monica Sorescu[1], Fatiha Benmokhtar[1], Douglas Higinbotham[2], Marcy Stutzman[2]

[1]Department of Physics, Duquesne University, Pittsburgh, USA
[2]Thomas Jefferson National Accelerator Facility, Newport News, Virginia, USA
Email: sorescu@duq.edu

Abstract

Six amorphous alloys (Alloy 1: $Fe_{56}Co_{24}Nb_4B_{13}Si_2Cu_1$, Alloy 2: $Fe_{68.5}Co_5Nb_3Cu_1Si_{15.5}B_7$, Alloy 3: $Fe_{75.3}Ni_{0.8}Cr_{0.9}Si_{8.7}B_{14.3}$, Alloy 4: $Fe_{56}Co_{24}Cr_{10}Nb_4B_3Si_1Cu_2$, Alloy 5: $Fe_{72.9}Nb_3Cu_1Si_{16.2}B_{6.9}$, Alloy 6: $Fe_{83.3}Si_{8.6}Nb_{5.5}B_{1.4}Cu_{1.2}$) were selected in terms of their composition and magnetostriction constants and uniformly irradiated in a high radiation environment in Hall A of the Thomas Jefferson National Accelerator Facility. The 2 GeV electron beam irradiation-induced effects were characterized by Mössbauer spectroscopy. The microstructural changes were related to the evolution of the hyperfine magnetic field distributions and isomer shifts. In particular, the occurrence of stress centers in the amorphous materials was evidenced.

Keywords

Metallic Glasses, Hyperfine Interactions, Magnetostriction, Radiation Effects, Mössbauer Spectroscopy

1. Introduction

To date, irradiation-induced effects have been considered in order to understand the relationship between magnetic behavior and select variation in the structural characteristics of materials [1]-[10]. Mostly, crystalline materials were subject to irradiation with electron beams [11]-[20] and discussed in terms of phenomenological models in which the underlying microstructure played an essential role.

In particular, electron-beam irradiation of amorphous alloys attracts nowadays considerable interest due to the emphasis on the structure-property relationships relevant to rational construction of new magnetic materials. However,

this irradiation study [21] was limited to 7 MeV electrons and it makes sense to explore the changes induced by GeV electrons. In these current investigations we study the irradiation-driven modifications induced by 2 GeV electrons in several advanced metallic glasses.

2. Materials and Methods

Amorphous ferromagnetic alloys (Alloy 1: $Fe_{56}Co_{24}Nb_4B_{13}Si_2Cu_1$, Alloy 2: $Fe_{68.5}Co_5Nb_3Cu_1Si_{15.5}B_7$, Alloy 3: $Fe_{75.3}Ni_{0.8}Cr_{0.9}Si_{8.7}B_{14.3}$, Alloy 4: $Fe_{56}Co_{24}Cr_{10}Nb_4B_3Si_1Cu_2$, Alloy 5: $Fe_{72.9}Nb_3Cu_1Si_{16.2}B_{6.9}$, Alloy 6: $Fe_{83.3}Si_{8.6}Nb_{5.5}B_{1.4}Cu_{1.2}$) were obtained from Spang Co. in ribbon form (compositions following the Finemet generation). The foils were exposed to the prompt high radiation environment created by a 2 GeV electron beam incident on a foil of Pb as part of the PREX-II experiment [22]. The foils all received a uniform dose of 0.1 Mrad of ionizing radiation as determined using special dosimeters located with the foils.

Room temperature Mössbauer spectroscopy measurements were performed with a SeeCo constant acceleration spectrometer using a ^{57}Co gamma ray source diffused in an Rh matrix. The spectra were analyzed with the WINormos-DIST package of programs, which was able to detail the hyperfine magnetic field distributions extracted from the spectra.

3. Results

Figure 1 shows the transmission Mössbauer spectra of alloys 1 and 2 after irradiation with 2 GeV electron beam at a radiation dose of 0.1 MRad, along with the hyperfine magnetic field distributions and isomer shift values extracted from the spectra during least-squares fitting.

The broad resonances in the Mössbauer spectra are due to the occurrence of fluctuations in the exchange interactions between the neighboring atoms, which cause the appearance of distributions of hyperfine parameters. The average values of the hyperfine magnetic field <BHF> are 24.94 and 20.97 T for alloys 1 and 2, respectively which is a typical range of parameter values for metallic glasses.

The relative intensity of lines 2 to 1 in the Mössbauer spectra (the magnetic texture parameter) is given by $R_{21} = 4\sin^2\theta/3[1 + \cos^2\theta]$, where θ is the angle between the direction of propagation of the gamma radiation and the direction of the hyperfine magnetic field. The θ values are 26.3° and 45.0° for alloys 1 and 2, respectively which indicate a rotation of the magnetic moments towards an out-of-plane orientation in the irradiated specimens. This result is consistent with the formation of stress centers, which are able to determine changes in direction for the magnetic moments in the ribbons. This idea is also supported by the hyperfine magnetic field distribution extracted from the Mössbauer spectrum of irradiated alloy 2, which is bimodal: it has a low-field component, which is consistent with the occurrence of atomic rearrangements and onset of chemical short-range order. The average isomer shift value <ISO>, also determined by

107
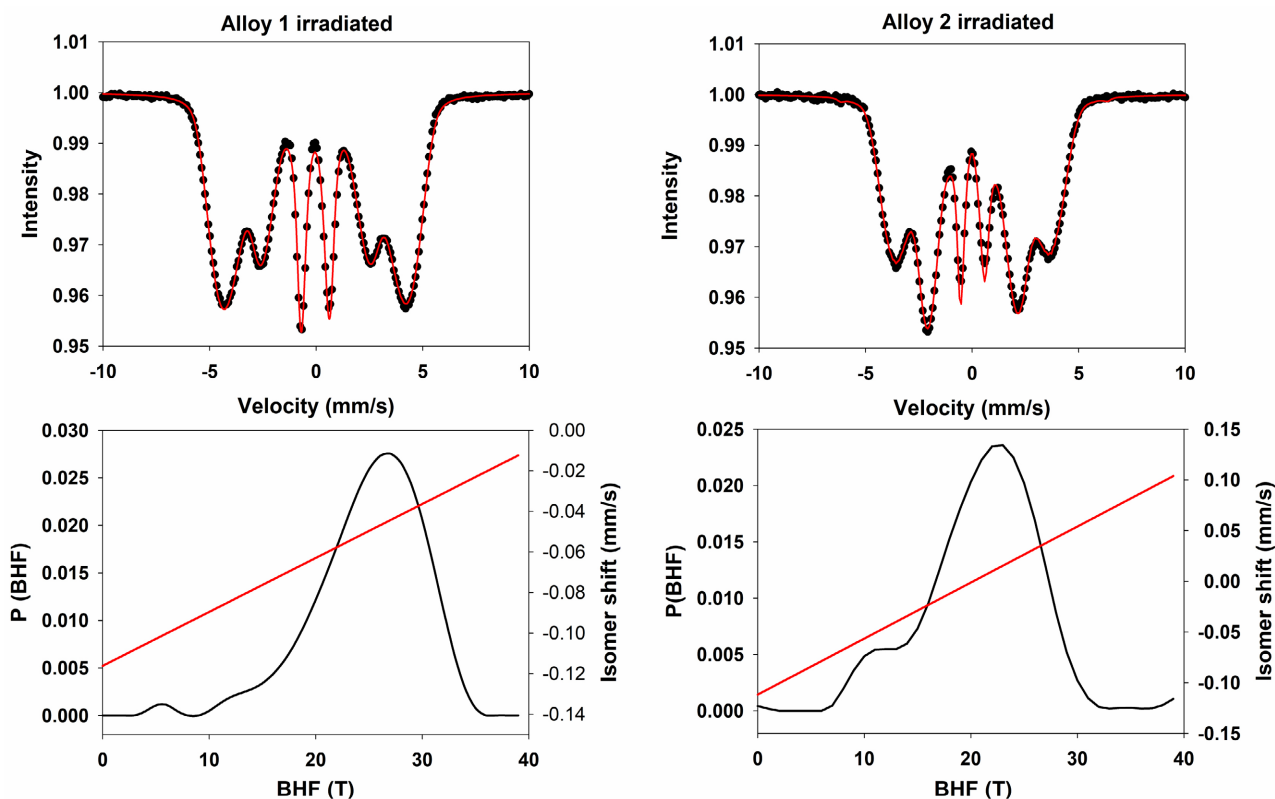
Figure 1. Mössbauer spectra of alloys 1 and 2 after 2 GeV e-beam irradiation.

the nonlinear least-square fitting procedure, is equal to -0.049 and 0.0041 mm/s for irradiated alloys 1 and 2, respectively. The corresponding values of as-quenched amorphous specimens before irradiation were $\langle BHF \rangle = 24.82$ and 21.07 T, $\theta = 26°$ and $45.5°$, and $\langle ISO \rangle = -0.050$ and 0.0044 mm/s, respectively. The formation of stress centers in the irradiated materials can tentatively be related to magnetostriction (alloy 1 has $\lambda_s = 20$ ppm), but it should be observed that the defects are also formed in alloy 2, which is a zero-magnetostriction composition.

Figure 2 shows the room temperature Mössbauer spectra of alloys 3 and 4 after 2 GeV electron beam irradiation. The average values of the hyperfine magnetic field are 22.95 and 16.11 T for alloys 3 and 4, respectively.

It can be observed that the width of the hyperfine magnetic field distribution is increased, the distribution having an enhanced low-field component which indicates the occurrence of changes in the chemical short-range order and atomic rearrangements in the amorphous structure. This is supported by the values obtained for the magnetic texture parameter, $R_{21} = 0.98$ and 0.74 for alloys 3 and 4, respectively. The corresponding values of the canting angle are $\theta = 57.9°$ and $45.5°$, which are consistent with an average overall in-plane orientation of the magnetic moment directions. This indicates the formation of stress centers, which are able to redirect the orientation of magnetic moments in the samples. The average isomer shift values are $\langle ISO \rangle = -0.0073$ and -0.098 mm/s for alloys
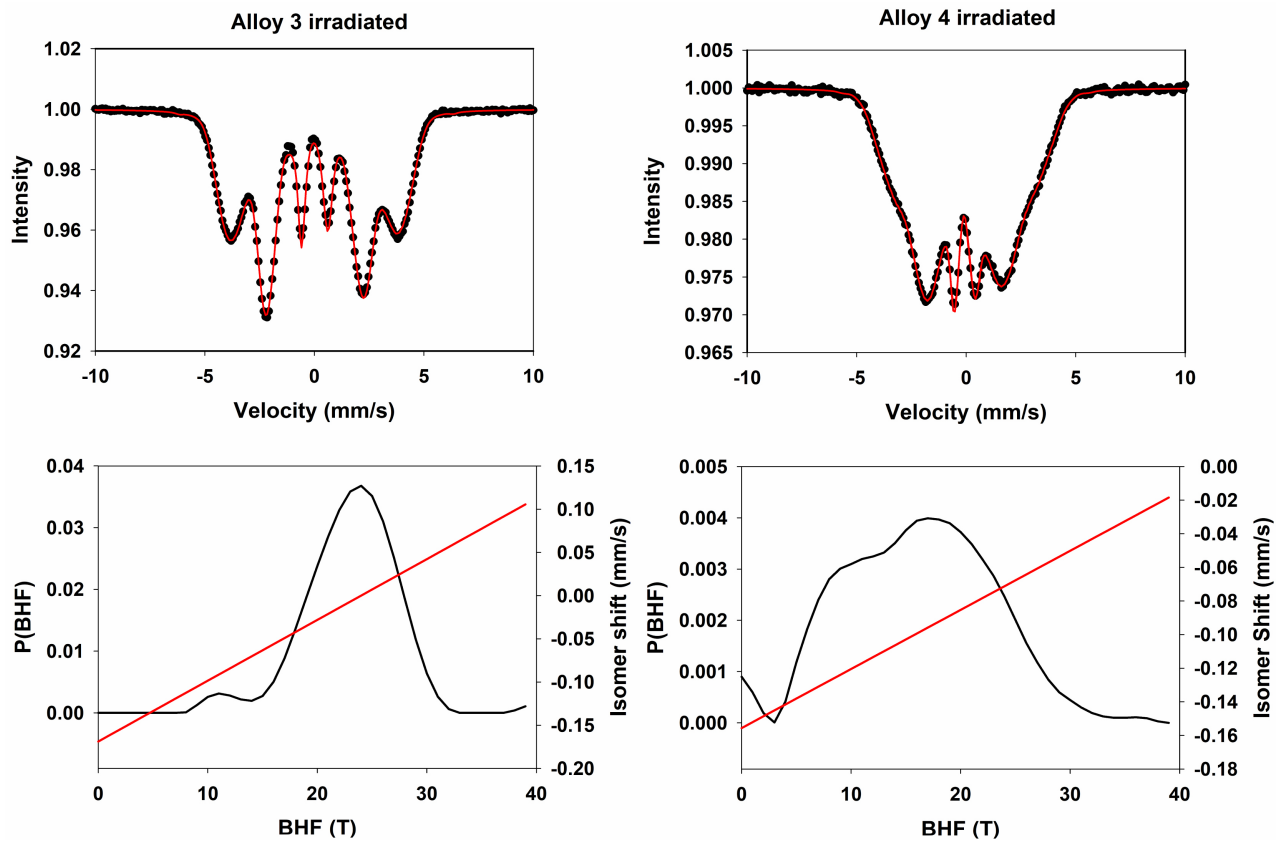
Figure 2. Mössbauer spectra of alloys 3 and 4 after 2 GeV e-beam irradiation.
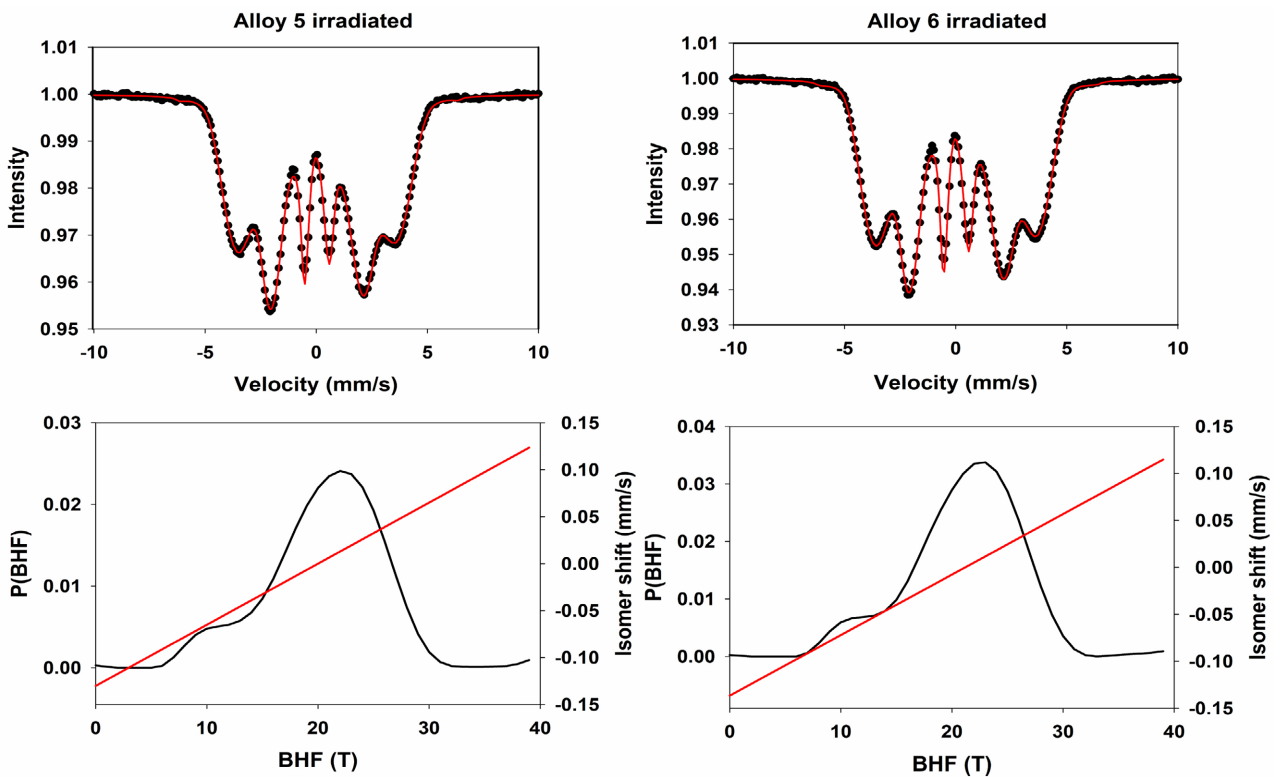
Figure 3. Mössbauer spectra of alloys 5 and 6 after 2 GeV e-beam irradiation.

3 and 4, respectively, which is consistent with changes in the electronic charge distribution at the nuclei, caused by the modifications in the chemical short-range order induced by electron beam irradiation.

Figure 3 displays the room-temperature Mössbauer spectra of alloys 5 and 6 after 2 GeV electron irradiation. The hyperfine magnetic field distributions had the average values of <BHF> = 20.55 and 21.08 T for alloys 5 and 6, respectively, with an increased width due to a small low-field component of the distribution.

This is consistent with sizeable migration of atoms in the amorphous matrix, but it should be noted that bulk crystallization of the specimens did not occur.

The magnetic texture parameter takes values R_{21} = 0.72 and 0.67, with average canting angles of 44.5° and 41.9°, which are close to a random orientation of magnetic moment directions. Alloy 5 has a negative magnetostriction constant, fact which demonstrates that stress centers are also formed in samples of negative λ_s due to magnetostriction. The average isomer shift had the values <ISO> = 0.0035 and 0.006 mm/s for alloys 5 and 6, which is consistent with the occurrence of variations in the chemical short-range order in the irradiated specimens.

4. Discussion and Conclusions

The present study sheds light on the fundamental effects underlying the interaction of high-energy electron beams with advanced metallic glasses. The formation of stress centers around defects induced by irradiation was demonstrated. Since the specimens remain in the amorphous phase, the development of radiation-resistant materials is encouraged.

Due to the thickness of the ribbon foils, the use of transmission electron microscopy is not possible. Scanning electron microscopy does not provide helpful information either, since irradiation is not a surface effect. Unlike low energy electrons, which leave their energy in the sample and induce bulk crystallization [21] [23], high energy electrons just pass through the sample and leave defects behind. Therefore, Mössbauer spectroscopy proves to be a powerful, high-resolution technique when used to investigate minute changes in the structure and properties of magnetic materials.

Acknowledgements

Conflicts of Interest

The authors declare no conflicts of interest regarding the publication of this paper.

References

[1] Mostaed, A., Balakrishnan, G., Lees, M.R. and Beanland, R. (2018) Electron-Irradiation Defects in $Yb_2Ti_{2.05}O_7$. *Acta Materialia*, **143**, 291-297. https://doi.org/10.1016/j.actamat.2017.10.028

[2] Nagase, T., Takizawa, K., Wakeda, M., Shibutani, Y. and Umakoshi, Y. (2010) Electron-Irradiation-Induced Solid-State Amorphization Caused by Thermal Relaxation of Lattice Defects. *Intermetallics*, **18**, 441-450. https://doi.org/10.1016/j.intermet.2009.09.003

[3] Shono, Y. and Oka, T. (2000) Complex Defects in Electron-Irradiated ZnS. *Journal of Crystal Growth*, **210**, 278-282. https://doi.org/10.1016/S0022-0248(99)00696-X

[4] Okada, A., Maeda, H., Hamada, K. and Ishida, I. (1999) Defect Structure Development in a Pure Iron and Dilute Iron Alloys Irradiated with Neutrons and Electrons. *Journal of Nuclear Materials*, **271**-**272**, 133-138. https://doi.org/10.1016/S0022-3115(98)00703-X

[5] Yasuda, K., Kinoshita, C., Matsumura, S. and Ryazanov, A.I. (2003) Radiation-Induced Defect Clusters in Fully Stabilized Zirconia Irradiated with Ions and/or Electrons. *Journal of Nuclear Materials*, **319**, 74-80. https://doi.org/10.1016/S0022-3115(03)00136-3

[6] Druzhkov, A.P. and Nikolaev, A.L. (2011) Effects of Solute Atoms on Evolution of Vacancy Defects in Electron-Irradiated FeCr-Based Alloys. *Journal of Nuclear Materials*, **408**, 194-200. https://doi.org/10.1016/j.jnucmat.2010.11.036

[7] Ortiz, C.J., Terentyev, D., Olsson, P., Vila, R. and Malerba, L. (2011) Simulation of Defect Evolution in Electron-Irradiated Dilute FeCr Alloys. *Journal of Nuclear Materials*, **417**, 1078-1081. https://doi.org/10.1016/j.jnucmat.2010.12.188

[8] Lee, H.S., Okada, H., Wakahara, A., Ohshima, T., Itok, H., Kawakita, S., Imaizumi, M., Matsuda, S. and Yoshida, A. (2003) 3 MeV Electron Irradiation-Induced Defects in $CuInSe_2$ Thin Films. *Journal of Physics and Chemistry of Solids*, **64**, 1887-1890. https://doi.org/10.1016/S0022-3697(03)00109-4

[9] Wang, D.K., Chen, B.K., Wei, Z.P., Fang, X., Tang, J.L., Fang, D., Aierken, A., Wang, X.H., Malyia, H.N. and Guo, Q. (2019) Electron Irradiation-Induced Defects and Photoelectric Properties of Te-Doped GaSb. *Journal of Physics and Chemistry of Solids*, **132**, 26-30. https://doi.org/10.1016/j.jpcs.2019.04.015

[10] Zhao, Y.W., Dong, Z.Y. and Deng, A.H. (2006) Electron Irradiation-Induced Defects in InP Pre-Annealed at High Temperature. *Materials Science in Semiconductor Processing*, **9**, 380-383. https://doi.org/10.1016/j.mssp.2006.01.021

[11] Yasunaga, K., Yasuda, K., Matsumura, S. and Sonoda, T. (2006) Nucleation and Growth of Defect Clusters in CeO_2 Irradiated with Electrons. *Nuclear Instruments and Methods in Physics Research B*, **250**, 114-118. https://doi.org/10.1016/j.nimb.2006.04.091

[12] Dudarev, S.L., Derlet, P.M. and Woo, K.H. (2007) Driven Mobility of Self-Interstitial Defects under Electron Irradiation. *Nuclear Instruments and Methods in Physics Research B*, **256**, 253-259. https://doi.org/10.1016/j.nimb.2006.12.013

[13] Wang, Q.Y., Geng, H.B., Sun, C.Y., Zhang, Z.H. and He, S.Y. (2010) Evolution of Defects in a Multicomponent Glass Irradiated by 1 MeV Electrons. *Nuclear Instruments and Methods in Physics Research B*, **268**, 1478-1481. https://doi.org/10.1016/j.nimb.2010.01.028

[14] Tuomisto, F., Look, D.C. and Farlow, G.C. (2007) Defect Studies in Electron-Irradiated ZnO and GaN. *Physica B*, **401**-**402**, 604-608.

https://doi.org/10.1016/j.physb.2007.09.032

[15] Babaee, S. and Ghozati, S.B. (2017) The Study of 1 MeV Electron Irradiation Induced Defects in N-Type and P-Type Monocrystalline Silicon. *Radiation Physics and Chemistry*, **141**, 98-102. https://doi.org/10.1016/j.radphyschem.2017.06.012

[16] Yeritsyan, H.N., Sahakyan, A.A., Grigoryan, N.E., Harutyunyan, V., Arzumanyan, V.K., Tsakanov, V.M., Grigoryan, B.A., Amatuni, G.A. and Rodes, C.J. (2020) Introduction Rates of Radiation Defects in Electron Irradiated Semiconductor Crystals of n-Si and n-GaP. *Radiation Physics and Chemistry*, **176**, Article ID: 109056. https://doi.org/10.1016/j.radphyschem.2020.109056

[17] He, M.R., Wang, S., Jin, K., Bei, H., Yasuda, K., Matsumura, S., Higashida, K. and Robertson, I.M. (2016) Enhanced Damage Resistance and Novel Defect Structure of CrFeCoNi under *in Situ* Electron Irradiation. *Scripta Materialia*, **125**, 5-9. https://doi.org/10.1016/j.scriptamat.2016.07.023

[18] He, M.R., Wang, S., Jin, K., Bei, H., Yasuda, K., Matsumura, S., Higashida, H.K. and Robertson, I.M. (2019) A Comparative Characterization of Defect Structure in NiCo and NiFe Equimolar Solid Solution Alloys under *In Situ* Electron Irradiation. *Scripta Materialia*, **166**, 96-101. https://doi.org/10.1016/j.scriptamat.2019.03.008

[19] Zardas, G.E., Symeonides, C.I., Euthymiou, P.C., Papaioannou, G.J., Yannakopoulos, P.H. and Vesely, M. (2008) Electron Irradiation Induced Defects in Undoped and Te-Doped Gallium Phosphide. *Solid State Communications*, **145**, 332-336. https://doi.org/10.1016/j.ssc.2007.12.003

[20] Hernandez-Fenollosa, M.A., Damonte, L.C., Mari, B. (2005) Defects in Electron Irradiated ZnO Single Crystals. *Superlattices and Microstructures*, **38**, 336-343. https://doi.org/10.1016/j.spmi.2005.08.027

[21] Sorescu, M., Knobbe, E.T. and Barb, D. (1995) Evolution of Phases and Microstructure in $Fe_{81}B_{13.5}Si_{3.5}C_2$ Metallic Glass during Electron-Beam and Pulsed-Laser Irradiation. *Physical Review B*, **51**, 840-850. https://doi.org/10.1103/PhysRevB.51.840

[22] Adhikari D., *et al.* (2021) Accurate Determination of the Neutron Skin Thickness of 208Pb through Parity-Violation in Electron Scattering. *Physical Review Letters*, **126**, Article ID: 172502. https://doi.org/10.1103/PhysRevLett.126.172502

[23] Sorescu, M. (2020) Recent Applications of the Mössbauer Effect. Dorrance Publishing Co., Pittsburgh.